Chapter 1

Introduction

1.1 Turbulence

The turbulent motion of fuids is still an unsolved problem, while it is a widely distributed appaerence dominating the practical fluid mechanics. The importance of understanding the motion called turbulence follows from its presence in a lot of cases of moving gases and liquids, one can say the majority of all real flows [34]. In engineering one has primarily the flow inside and around technical apparatusus in mind. These flows can be distinguished into a few fundamental types:

- Turbulence while flow through grids (wind tunnel turbulence)
- Flows in pathways (pipes, ducts, channels)
- Free turbulence (Jets, wake flows, areas of mixing)
- Near wall flows (Boundary layers)
- Apart from that the most geophysical flows occur to be turbulent. Those are atmospheric flow, flows in rivers, tides and many more. Also the flow in a climatised room behaves turbulent.
- Also in astrophysics turbulent flows are observable in the chromosphere and star atmosphere while it also plays a crucial role for the development of spiral galaxies and the processes in accretion disks.

The turbulent motion appeals in versatile manners. For example the viscous drag acting on surfaces overflown is much higher for turbulent compared to laminar flow, and it follows different physical laws. On the other hand turbulence can suppress an early

separation of the boundary layer, resulting in a reduction of the friction. A fundamental characteristic of turbulent flows is the intense mixing of liquids and/or gases in order that impurities (i.e. dye in water, smoke in air) are rapidly distributed across the volume, mass and heat transfer is huge for turbulent flows. Turbulent flows can cause vibrations at solid body's like wind around buildings. The gust load for air vehicles results from the atmospheric turbulence. Acoustic sound waves passing through turbulent flow experience a scattering and the pressure fluctuations in turbulent flows of high velocities can represent strong acoustic sources, being a serious task for aviation and vehicle aerodynamics.

To give a concisely definition for the understanding what turbulent flow is, is far from simple. The following characteristics can be used to depict turbulent flows:

- 1. *Turbulent flows proceed irregular and unsteady,* such as the velocity variates complicated with space and time. Thus, a single measurement can not deliver a reproducable result, but provide a statistical fluke.
- 2. *Turbulent flows are vortex dominated*
- 3. *Turbulent flows are three dimensional*
- 4. *Turbulent flows are instationary*

The properties given in 3 and 4 are resulting from the irregularity given in 1. Flows not representable by these characteristics are not considered to be turbulent. For example the so called van Kármán street, the flow behind a cylindrical body, is vortex dominated but due to its regularity one does not count it as a turbulent flow. Furthermore the vortex flows generated by the seperation of stream lines at sharp edges are not generally turbulent. At the other hand it exists areas near turbulent flows experiencing velocity fluctuations excited from the pressure fluctuations of the turbulent flow, which are eddy-free and thus, these areas are understood to be non turbulent. As an example for turbulent flow in Figure 1.1 an image of the turbulent atmosphere of the Jupiter is depicted.

A liquid or gas, seen as a continuum, is a mechanical system of infinite degree of freedom. The motions of the fluid particles at different locations in space and time are coupled by the differential equations of fluids, but, in consequence of instability a random encounter of apparently not related circumstances under certain conditions results in an infinite diversity of motions. Such processes where the velocities are random functions of space and time are called stochastic processes. Thus, turbulent flows are understood to be stochastical processes.

As turbulent flows are vortex dominated, the rotation deviates from Zero ($\nabla \times u \neq 0$), it results that viscous forces are not negligible.

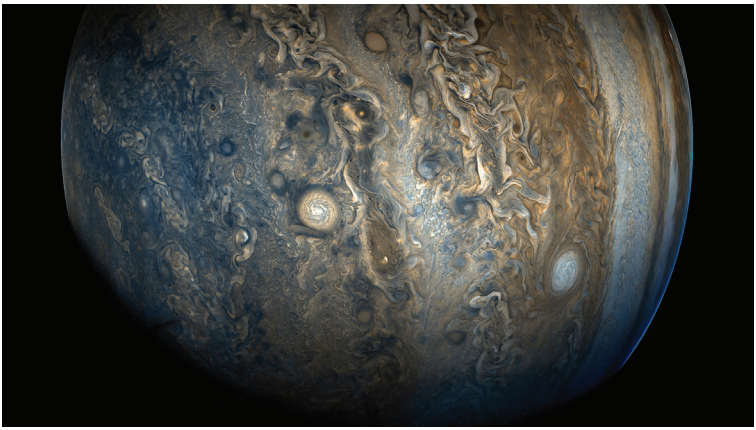

FIGURE 1.1: Turbulence in Atmospheres: Jupiter's southern hemisphere in detail, image taken by NASA's Juno spacecraft. The colour-enhanced view captures one of the white ovals in the "String of Pearls," one of eight massive rotating storms at 40 degrees south latitude on the gas giant planet. The image was taken on Oct. 24, 2017 at 11:11 a.m. PDT (2:11 p.m. EDT), as Juno performed its ninth close flyby of Jupiter. The spatial scale in this image is $22.3 km/px$. Citizen scientists Gerald Eichstädt and Seán Doran processed this image using data from the JunoCam imager. Image Credits: NASA/JPL-Caltech/SwRI/MSSS/Gerald Eichstädt/ Seán Doran, Source: $https://www.nasa.gov/mission_pages/juno/images/index.html$, at 24.10.18

A famous example of flow instability occurs between two concentric cylinders of radii R_1, R_2 and length L, rotating independently with the angular velocities Ω_1 and Ω_2. In case of differential rotation angular momentum is transported between the cylinders. The so called Taylor-Couette (TC) flow is of fundamental interest in terms of transport properties in rotating systems, as Earth's atmosphere or accretion disks in case of Rayleigh stable flows or industrial applications such as journal bearings for Rayleigh instable flows. A better understanding of the transport processes and the turbulent structures and a uniform description of these complex aspects, these are tasks of great importance for many research areas van Gils et al. [38]. The aim of this thesis is to experimentally investigate the turbulent Taylor-Couette flow for radius ratio $\eta = 0.5$ at high shear Reynolds numbers and rotation of inner as well as outer cylinder.

For the present investigation fundamental scientific questions were raised on the topic of turbulent Taylor-Couette flow.

- *How large is the angular momentum flux for given flow conditions?*

- *Does the angular momentum flux scale with Reynolds number comparable with other canonical flows?*
- *Do Taylor-vortices exist for large Reynolds numbers?*
- *How does the counter-rotation affects the turbulent Taylor-Couette flow?*

The scope of the experimental study is also limited. The main limitation is the given radius ratio $\eta = 0.5$, which holds for the whole investigation. In parallel also investigations for other radius ratios were performed for more narrow gap: $\eta = 0.71$ investigations were made but have been excluded from this thesis. For wider gaps $\eta < 0.5$ the flow is also analysed and will be the scope of future studies. The shear Reynolds numbers were limited by the maximal driving velocities and reached up to $Re_S < 1.3 \cdot 10^6$. Also the investigation had the scope on centrifugally instable flows, so the behaviour in the Rayleigh-stable regime is not included in this thesis.

1.2 Outline of the thesis

The outline of the thesis is as follows. Chapter 2 explains the physical background on turbulent Taylor-Couette flow which is important for the understanding of the study. Chapter 3 gives details of the two Taylor-Couette experiments built up for this study and explains the principles of the measurement techniques used. In one of the experiments an accurate torque measurement unit was specially designed and implemented. The results of the torque measurements are discussed in Chapter 4.

Chapter 5 consists of velocity measurements by the use of Laser Doppler Velocimetry (LDV) and Particle Image Velocimetry (PIV) revealing statistical velocity profiles in the system. In Chapter 6 a detailed flow visualisation follows. Here the flow behaviour in the concentric gap was analysed qualitively and gives a brief understanding of what kind of structures happen in the Taylor-Couette system and what will be needed for further investigations. The further investigation, in Chapter 7, is directly attached to the flow visualisation. By the use of the same equipment a Particle Image Velocimetry is performed for the flow close to the outer cylinders wall. Here the angular and axial velocities are measured in a short azimuthal and long axial area of interest.

Chapter 8 finally reports a Particle Image Velocimetry at different horizontal planes. From these measurements the three dimensional meanflow can be analysed. The measurements finally give the ability to understand the contributions of the different flow structures onto the angular momentum flux. Chapter 9 finally concludes all over the thesis.

Chapter 2

Theoretical background and theoretical approach

To describe physical system one needs to derive the underlying laws of conservation. In our case we want to investigate the flow of a fluid in rotation. The important laws of conservation in this case are the conservation of mass and momentum. The influence of heat is negligible in this case, so one does need to care about the conservation of energy. In the following chapter the conservation of mass and momentum are used in cylindrical coordinates, using this the Continuity equation and the Navier-Stokes-equation are derived for the Taylor-Couette system.

2.1 Fluid in motion

To describe a fluid in motion in mathematical way one needs a fundamental set of equation. For incompressible fluids, such as we look at the system variables are the velocity field and the pressure distribution. This can be solved taking two conservations laws, the conservation of mass and the conservation of momentum. For fluids these equations become special names: The continuity equation:

$$\frac{\partial \rho}{\partial t} + \nabla \cdot (\rho \vec{u}) = 0 \tag{2.1}$$

with the density ρ, and velocity u. For incompressible fluid $\rho = const.$ it becomes:

$$\nabla \cdot \vec{u} = 0 \tag{2.2}$$

Formulating the momentum balance for fluid flows the Navier-Stokes equation can be written as:

$$\frac{\partial \vec{u}}{\partial t} + (\vec{u}\nabla)\vec{u} = -\frac{1}{\rho}\nabla p + \nu\nabla^2\vec{u} + \vec{f} \tag{2.3}$$

with the pressure p, kinematic viscosity $\nu = \frac{\mu}{\rho}$, dynamic viscosity μ and probable external force fields $\vec{f}$. As one is interested in rotating flows between concentric cylinders the cylindrical coordinates are used. The Nabla and Laplace operator are written as follows.

$$\nabla = \frac{\partial}{\partial r} + \frac{1}{r}\frac{\partial}{\partial \varphi} + \frac{\partial}{\partial z} \tag{2.4}$$

$$\nabla^2 = \frac{\partial^2}{\partial r^2} + \frac{1}{r}\frac{\partial}{\partial r} + \frac{1}{r^2}\frac{\partial^2}{\partial \varphi^2} + \frac{\partial^2}{\partial z^2} \tag{2.5}$$

Thus, the Navier-Stokes equations of an incompressible fluid in cylindrical coordinates reads as:

$$\frac{\partial u_r}{\partial t} = -(\vec{u}\cdot\nabla)u_r + \frac{u_\varphi^2}{r} - \frac{1}{\rho}\frac{\partial p}{\partial r} + \nu\left(\nabla^2 u_r - \frac{u_r}{r^2} - \frac{2}{r^2}\frac{\partial u_\varphi}{\partial \varphi}\right), \tag{2.6}$$

$$\frac{\partial u_\varphi}{\partial t} = -(\vec{u}\cdot\nabla)u_\varphi + \frac{u_r u_\varphi}{r} - \frac{1}{\rho}\frac{\partial p}{\partial \varphi} + \nu\left(\nabla^2 u_\varphi - \frac{u_\varphi}{r^2} - \frac{2}{r^2}\frac{\partial u_r}{\partial \varphi}\right), \tag{2.7}$$

$$\frac{\partial u_z}{\partial t} = -(\vec{u}\cdot\nabla)u_z - \frac{1}{\rho}\frac{\partial p}{\partial z} + \nu\nabla^2 u_z \tag{2.8}$$

The differential operators in these equations on a scalar field Φ are given as:

$$(\vec{u}\cdot\nabla)\Phi = \left(u_r\frac{\partial}{\partial r} + \frac{u_\varphi}{r}\frac{\partial}{\partial \varphi} + u_z\frac{\partial}{\partial z}\right)\Phi \tag{2.9}$$

External force fields can be neglected in our case. If one wants to write the Navier-Stokes equation 2.10 in dimensionless form (all dimensionless variables are noted by index u_* it becomes:

$$\frac{\partial \vec{u}_*}{\partial t_*} + (\vec{u}_*\nabla_*)\vec{u}_* = -\frac{1}{\rho}\nabla_* p_* + \frac{\nu}{LU}\nabla_*^2\vec{u}_* + \vec{f}_* \tag{2.10}$$

were L is a characteristic length and U a characteristic velocity. The dimensionless parameter $Re := \frac{UL}{\nu}$ is called the Reynolds number.

2.2 Taylor-Couette flow

The geometry of the Taylor-Couette system is simple. Two concentric cylinders of Radii $R_{1,2}$ rotate with angular velocities Ω_1, Ω_2, where the indices 1 and 2 denote the inner and outer cylinder respectively, are the boundaries of the geometry. In respect to this a key parameter is the radius ratio $\eta = R_1/R_2$, while the gap width $d = R_2 - R_1$ is a characteristic scale of the system and been used for calculating dimensionless properties.

In a theoretical approach the system has infinite length. In Reality the system has to have axial borders in the form of end plates. The length between the end plates L can be measured in gap widths.

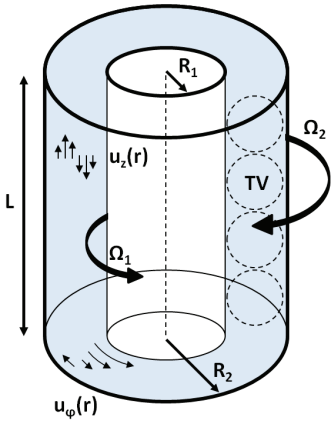

FIGURE 2.1: Sketch of the Taylor-Couette flow: The flow in the gap between two concentric, coaxial cylinders of Radii R_1 (inner) and R_2 (outer cylinde) and length L rotating with angular velocities Ω_1, Ω_2.

Thus, important parameters of the TC system are the radius ratio $\eta = R_1/R_2$, the aspect ratio $\Gamma = L/d$ with the gap width $d = R_2 - R_1$ and the ratio of angular velocities $\mu = \Omega_2/\Omega_1$. To characterize the flow in the gap, one can derive two Reynolds numbers related to the inner (1) and outer (2) rotation , $Re_{1,2} = R_{1,2}\Omega_{1,2}d/\nu$, with the kinematic viscosity ν of the fluid. In analogy to other shear flows a shear Reynolds number can be defined as $Re_S = \frac{2}{1+\eta}|Re_1 - \eta Re_2| = \frac{2R_2R_1d}{(R_2+R_1)\nu}|\Omega_2 - \Omega_1|$ [9], which differs from the one introduced in [37] for the boundary layers.

2.2.1 Transport of angular motion

Recently Eckhardt et al. [10, 11] derived a theory on torque scaling in TC flow. This theory describes the transverse current of azimuthal motion J_ω that is constant over all radii with

$$J_\omega = r^3(\langle u_r\omega\rangle_{A,t} - \nu\partial_r\langle\omega\rangle_{A,t}), \tag{2.11}$$

where $\omega = u_\varphi/r$ is the local angular velocity and the brackets $\langle\ \rangle_{A,t}$ denote a mean over a cylindrical surface at radius r and over time. The cylinders are impermeable so the radial velocity and the first term of the equation equal zero at the boundaries ($u_r(r = R_1, R_2) = 0$). At this radial position the second term is proportional to the

torque T that the fluid experiences at the boundary. Hence, measuring the dimensionless torque $G = T/(2\pi L\rho\nu^2)$ at the rotating inner or outer cylinder corresponds to measuring the current $J_\omega = \nu^2 G$. This theory is in close analogy to the Grossmann-Lohse theory on Rayleigh-Bénard flow (RB) [14] and denotes several analogies between the systems [10, 11]. Corresponding to the heat transport Nusselt number in RB one defines a quasi-Nusselt number of TC flow $\mathrm{Nu}_\omega = G/G_{lam}$, where $G_{lam} = R_1 R_2 Re_S d^{-2}$ is the dimensionless torque of the analytical Couette solution.

This torque has been measured in the past and has been scaled with the Reynolds number Re_1. Wendt [39] measured the torque at the rotating inner cylinder for three different radius ratios $\eta = 0.68, 0.85, 0.935$ and Reynolds numbers between $50 \leq Re_{1,2} \leq 10^5$. He fitted the dimensionless torque to power laws $G = Re^\alpha$ with $\alpha = 1.5$ for $400 \leq Re_1 \leq 10^4$ and $\alpha = 1.7$ for $10^4 \leq Re_1 \leq 10^5$. Lathrop et al. [20], using a radius ratio of $\eta = 0.724$ for a Reynolds number range of 10^3 to 10^6 and $\mu = 0$, found that the scaling exponent α of the torque still monotonically increases from 1.66 to 1.87 - beyond a critical Reynolds number of 1.3×10^4. Lewis and Swinney [21] repeated these measurements with higher accuracy and verified the results. Later, Paoletti and Lathrop [30] revised the experiment and measured the torque for various flow situation of counter- and co-rotating cylinders. For measurements at a constant shear Reynolds number Re_S they observed a peak in the torque data for a counter-rotation corresponding to $\mu_{max} = -0.33$ for $\eta = 0.725$. Furthermore, the Twente turbulent Taylor-Couette experiment (T^3C) [17, 37, 38] is used to investigate the state of ultimate turbulence in TC flow. Their experiments show that the quasi-Nusselt number Nu_ω scales with the shear Reynolds number like $\mathrm{Nu}_\omega \sim {Re_S}^{0.78\pm0.03}$ [17, 38] for different investigated ratios of angular velocities μ. Recompensating this scaling ($\mathrm{Nu}_\omega \cdot {Re_S}^{-0.78}$) they obtain the dependency of Nu_ω on μ. They found a maximum at $\mu_{max} = -0.33 \pm 0.04$ for $\eta = 0.716$ as well. A collaborative work [31] shows how the data of the Maryland and Twente experiment coincide and the torque factorizes into $G = f(\mu)\, g(Re_S)$ as previously observed in [9, 30, 38]. But the question still remains, how do $f(\mu)$ and $g(Re_S)$ depend on the geometry of the Taylor-Couette systems? A first answer to this question was given by the Twente group by the conjecture that the angle bisector between the two Rayleigh stability lines could serve as a potential prediction for the location of the torque maximum in dependence on the radius ratio. This hypothesis is supported by their measured maximum at $\mu_{max} = -0.33$ and PIV data [17] for $\eta = 0.716$ [17, 37]. The experimental investigation for $\eta = 0.5$ in Merbold et al. [24] are in disagreement with this hypothesis. Brauckmann and Eckhardt [3] as well as the experimental investigations of various other η by Ostilla-Monico et al. [27] show that this prediction is also not valid for narrow gaps. Brauckmann and Eckhardt [3] explained the torque maxima by the enhanced large scale circulation using the analytical expression of the Taylor-Couette stability of Esser and Grossmann [12], for

relatively wide gaps this prediction holds with the experimental and numerical findings. We call this prediction for the location of the torque maxima dependent on radius ratio EG-prediction. For the radios ratio $\eta = 0.5$ different velocimetry studies were performed. Van der Veen et al. [36] performed Particle Image Velocimetry in the experiment in Cottbus for different flow behaviours supporting the EG-prediction. These measurements are summarized in Chapter 5. The measurements reported in Chapter 8 and also by Froitzheim et al. [13] were done in the same experiment and extended the parameter space. The experiments, in agreement with the EG-prediction, showed a strengthening of the vortices at the torque maxima while for pure inner cylinder rotation the energy of Taylor-Vortices vanishes for high Reynolds numbers. While the location of the maxima can be determined accurately by the EG-prediction the torque for a given set of rotations is still not predictable.

Chapter 3

The Cottbus Taylor-Couette experiments: Experimental setup and measurement techniques

3.1 Turbulent Taylor Couette Cottbus

To investigate the turbulent Taylor-Couette flow a specially designed experiment is used. A drawing and image of the experiment is shown in Fig. 3.1. The experiment has been used in a prior research project to investigate the influence of a radial temperature gradient onto Taylor-Couette flow. For the present study the experiment needed a crucial revision of the design (chapter 3.1.1). Prior the experiment was able to reach Reynolds numbers up to $Re_S < 10^5$ for inner cylinder rotation. The outer cylinder was kept at rest. To reach very high Reynolds numbers in the order of 10^6, the driving of the inner cylinder had to be changed (see chapter 3.1.3). Also an exchange of bearings and sealings became necessary. The outer cylinder as well as the end plates are now equipped with driving and gearbox. Different transmission ratios are applied to increase the usable range of angular velocities. As one is interested to measure the angular motion flux depending on the input parameters, the implementation of a torque measurement system inside the inner cylinder is a key advantage of this experiment and discussed in chapter 3.1.2.

3.1.1 Geometry and materials

The experimental investigations are carried out in a Taylor-Couette apparatus surrounded by a water bath box as shown in Fig. 3.2. The water bath box (5) and the outer